

## A GENERALIZED OPTIMAL SIGNAL PROCESSING ALGORITHM FOR FREQUENCY-STEPPED CW DATA

Shawkang M. Wu\*, Gary A. Ybarra\*\*, Winser E. Alexander\*

\* North Carolina State University, Dept. of Electrical and Computer Engineering, Raleigh, NC

\*\* Duke University Dept. of Electrical Engineering, Durham, NC

### ABSTRACT

We derive a complex non-linear optimal signal processing algorithm for estimating target reflection ranges from a set of frequency-stepped CW measurements. We demonstrate the performance of this algorithm using synthetic FSCW data through comparisons with the IFFT and the real version of the optimal signal processing algorithm.

### INTRODUCTION

The frequency-stepped continuous wave (FSCW) radar system has been used in reflection range estimation since the early '70's [1]. The physical data measured by the FSCW radar system is a sequence of complex reflection coefficients, which can be interpreted as samples of the radar channel frequency response  $H(j\omega)$ . The objective is to find the reflection range from these samples. The standard approach [2] is to apply the IFFT to these samples to obtain an estimate of the radar channel impulse response. The resolution of the IFFT is limited by the bandwidth. In applications where reflections occur in an inhomogeneous medium, such as a plasma [3], a narrow bandwidth is required to avoid significant dispersion, and the IFFT often fails to provide satisfactory resolution.

Ybarra et al. [3] presented an optimization algorithm for processing FSCW radar data and showed range resolution enhancement over the IFFT. This paper presents a generalized version of [3] in that the constraint on the amplitudes of the reflections has been relaxed to permit them to be complex. This change allows the reflection to be modeled as a wavelet rather than an abrupt discontinuity. The algorithm derived in this paper is general in the number of reflections. However, simulation results are presented for one and two reflections for the purpose of visually presenting the performance. In order to distinguish the two algorithms, we call the one in [3] the real algorithm, and the one in this paper the complex algorithm.

### DERIVATION

The complex algorithm minimizes the performance measure  $J$ ,

$$J = \sum_{i=1}^n |\mathbf{H}(j(\omega_0 + i\Delta\omega)) - \mathbf{H}_m(j(\omega_0 + i\Delta\omega))|^2 \quad (1)$$

where  $n$  is the number of reflection coefficients,  $\mathbf{H}_m(j(\omega_0 + i\Delta\omega))$  represent the measured reflection coefficients, and  $\mathbf{H}(j(\omega_0 + i\Delta\omega))$  represent the values of the theoretical model computed at the frequency of the measured reflection coefficients. The  $\mathbf{H}(j(\omega_0 + i\Delta\omega))$  are also samples of the frequency response of the time domain model

$$h(t) = A_1\delta(t-t_1) + A_2\delta(t-t_2) + \dots + A_m\delta(t-t_m) \quad (2)$$

$$H(j\omega) = A_1e^{-j\omega t_1} + A_2e^{-j\omega t_2} + \dots + A_m e^{-j\omega t_m} \quad (3)$$

where the  $A_i$  are the complex amplitudes, the  $t_i$  are the two-way time delays to the reflections, and  $m$  is the model order. Therefore,  $J$  is non-linear in  $t_i$ , and quadratic in  $A_i$ . The optimization problem is to find the  $A_i$  and  $t_i$  that minimize  $J$ . For each  $t_i$  in a pre-windowed range,  $J$  is minimized by solving for the  $A_i$  in closed form in the least squares sense [4]

$$\text{find } \mathbf{a} \text{ minimizing } \|\mathbf{Fa} - \mathbf{f}\|_2 \quad (4)$$

where  $\mathbf{F} \in C^{n \times m}$ ,  $\mathbf{a} \in C^{m \times 1}$ , and  $\mathbf{f} \in C^{n \times 1}$ . The complex matrix  $\mathbf{F}$  is composed of frequency response estimates based on the model (3), and the complex vector  $\mathbf{f}$  contains the physical frequency response measurements given by

$$\mathbf{f} = [ H_M(\omega_1) \quad H_M(\omega_2) \quad H_M(\omega_3) \quad \dots \quad H_M(\omega_n) ]^T \quad (5)$$

The complex vector  $\mathbf{a}$  in (4) is composed of reflection amplitudes  $A_i$  to be determined

$$\mathbf{a} = [ A_{1r} + jA_{1i} \quad A_{2r} + jA_{2i} \quad \dots \quad A_{mr} + jA_{mi} ]^T \quad (6)$$

The solution to (4) is found by minimizing the scalar that results from the following squared inner product

$$y = \|(\mathbf{Fr} + j\mathbf{Fj})(\mathbf{ar} + j\mathbf{aj}) - (\mathbf{fr} + j\mathbf{fj})\|^2 \quad (7)$$

where the subscripts  $\mathbf{r}$  and  $\mathbf{i}$  denote real and imaginary parts respectively. In order to solve for the vector  $\mathbf{a}$ , the gradient of (7) is taken with respect to  $\mathbf{ar}$  and  $\mathbf{aj}$  independently.

$$\begin{aligned} \frac{\partial y}{\partial a_r} &= 2(\mathbf{Fr}^T \mathbf{Fr} + \mathbf{Fj}^T \mathbf{Fj})\mathbf{ar} - 2(\mathbf{Fr}^T \mathbf{Fj} - \\ &\quad \mathbf{Fj}^T \mathbf{Fr})\mathbf{aj} - 2(\mathbf{Fr}^T \mathbf{fr} + \mathbf{Fj}^T \mathbf{fj}) = 0 \quad (8) \end{aligned}$$

$$\begin{aligned} \frac{\partial y}{\partial a_j} &= 2(\mathbf{Fr}^T \mathbf{Fr} + \mathbf{Fj}^T \mathbf{Fj})\mathbf{aj} - 2(\mathbf{Fj}^T \mathbf{Fr} - \\ &\quad \mathbf{Fr}^T \mathbf{Fj})\mathbf{ar} + 2(\mathbf{Fj}^T \mathbf{fr} - \mathbf{Fr}^T \mathbf{fj}) = 0 \quad (9) \end{aligned}$$

The result of this minimization process is a real, square set of simultaneous linear equations, and equations (8) and (9) can be re-written in a concise matrix form

$$\begin{bmatrix} \mathbf{A} & -\mathbf{B} \\ \mathbf{B} & \mathbf{A} \end{bmatrix} \begin{bmatrix} \mathbf{a}_r \\ \mathbf{a}_j \end{bmatrix} = \begin{bmatrix} \mathbf{C}_1 \\ \mathbf{C}_2 \end{bmatrix} \quad (10)$$

where  $\mathbf{A} = \mathbf{F}_r^T \mathbf{F}_r + \mathbf{F}_j^T \mathbf{F}_j$ ,  $\mathbf{B} = \mathbf{F}_r^T \mathbf{F}_j - \mathbf{F}_j^T \mathbf{F}_r$ ,  $\mathbf{C}_1 = \mathbf{F}_r^T \mathbf{f}_r + \mathbf{F}_j^T \mathbf{f}_j$ , and  $\mathbf{C}_2 = \mathbf{F}_r^T \mathbf{f}_j - \mathbf{F}_j^T \mathbf{f}_r$ . The complex algorithm utilizes the similar recursive procedure and grid search given in [3] to find the solution pairs  $A_i, t_i$  in (2). Readers should refer to [3] for detail.

## COMPUTATIONAL COMPLEXITY

The complex algorithm developed in the previous section can be applied directly to non real-time operations. However, for those applications requiring real-time operations, the computational cost of the complex algorithm has to be investigated. The number of floating point operations required to find one point in the  $J$  function is approximately

$$N_c = \frac{5}{2}m^2n + 19mn + 80m^3 \quad (11)$$

where  $m$  is the number of delays, and  $n$  is the number of physical measurements. The last term  $80m^3$  is due to the singular value decomposition [5] used to solve for  $\mathbf{a}_r$  and  $\mathbf{a}_j$  in (10). For a two delay case,  $N_c = 48n + 640$ . If the  $J$  function is well-behaved, the global minimum may be found in very few iterations of scanning both time axes. However, when  $m$  becomes large, parallel processing will be required to implement the algorithm in real time.

## EXPERIMENTAL RESULTS

The first set of data compares the performance between the IFFT, the real algorithm, and the complex algorithm. A sequence of 801 reflection coefficients spanning 14 to 18 GHz was created from a two reflection model with the time delays  $(t_1, t_2) = (2.0, 4.0)\text{ns}$ . Fig. 1, Fig. 2, and Fig. 3 show a comparison of the performance between the three algorithms.

The peaks in the plots correspond to the reflections, and their time delays correspond to the range estimation to the reflection. The three algorithms all produce accurate estimates at 2ns and 4ns. Due to the wide bandwidth, both optimization algorithms need only use one dimensional models to detect the reflections accurately. Fig. 2 shows a sinc envelope modulating a high frequency sinusoidal function. The modulation creates ambiguities in determining the time delay estimates. The analytical expressions for the  $J$  functions show that this phenomenon is eliminated by the complex algorithm.

$$J_r = \sum_{i=1}^n |r_i|^2 - \frac{1}{n} \left( \sum_{i=1}^n |r_i| \cos(\omega_i t_1 + \theta_i) \right)^2 \quad (12)$$

$$J_c = \sum_{i=1}^n |r_i|^2 - \frac{1}{n} \sum_{i=1}^n |r_i|^2 - \frac{2}{n} \sum_{i=1}^n \sum_{j=i+1}^n |r_i||r_j| \cos((\omega_i - \omega_j)t_1 + (\theta_i - \theta_j)) \quad (13)$$

where  $J_r$  and  $J_c$  are the  $J$  functions of the real and complex algorithms, respectively,  $|r_i|$  and  $\theta_i$  are the magnitude and phase angle of each measurement, respectively, and  $t_1$  is the time delay.

In the next set of data, 51 measurements were made from 14 to 14.25 GHz, while the delays were kept at 2 and 4 ns. The IFFT for this data set is shown in Fig. 4, where the two estimated reflections have merged into one, and hence, are not distinguishable.  $J_r$  and  $J_c$  for this case are shown in Fig. 5 and Fig. 6, respectively. Since the bandwidth is reduced to 250 MHz, two dimensional models for the optimization algorithms are required. In Fig. 5 there are two peaks at (1.05ns, 3.78ns) and (3.78ns, 1.05ns), but they are not accurate estimates. A zoomed version of Fig. 6 plotting those points below  $J = 0.1$  is shown in Fig. 7. It clearly shows two deep minima located at (2.0ns, 4.0ns). This experiment demonstrates the resolution enhancement offered by the complex algorithm over the IFFT and the real algorithm.

The data points for the IFFT have to be uniformly distributed, but there are applications such as radio astronomy [6] and machine vision [7], where data must be non-uniformly distributed. The complex algorithm can process non-uniformly sampled data with no increase in computational requirements. In order to demonstrate this feature, a sequence of 801 reflection coefficients were created from a model of four reflections with time delays  $t_1 = 1.5\text{ns}$ ,  $t_2 = 3.5\text{ns}$ ,  $t_3 = 4.5\text{ns}$ , and  $t_4 = 7.5\text{ns}$ . 21 points were uniformly sampled from this 801 points. The sampling rate is  $T = 1/\Delta f$ , where  $\Delta f = 4G/20$ . The IFFT for these 21 points is shown in Fig. 8 in which the last reflection at  $t_4 = 7.5\text{ns}$  has been aliased to 2.5ns. This is due to the fact that the sampling rate is 5ns and the IFFT is a periodic function. Any reflections located beyond 5ns will be aliased into this 0-5ns region. Therefore, unless we have *a priori* knowledge of the time delays, we would not be able to distinguish the actual reflections from the aliased versions.

The above aliasing effect can be reduced using non-uniformly sampled reflection coefficients [8]. A sampling procedure was developed

$$s_i = s_{i-1} + k(i-1) \quad (14)$$

where  $s_i$  is the index number of the reflection coefficient,  $k$  is an integer step number, and  $i$  runs from 1 to  $n$  such that  $s_n \leq$  total number of data points. We chose  $k = 3$  to obtain 23 non-uniformly sampled reflection coefficients from the above 801 data set.  $J_c$  for this case is shown in Fig. 9. The four peaks all show fairly accurate time delay estimates, but the third and fourth appear marginal in the depth of the pulses compared to the noisy side lobes. When  $t_i$  is expanded to 100ns,  $J_c$  is shown in Fig. 10 which shows clearly the first two reflections and a periodicity of  $T_j = 68.16 - 1.50 = 66.66\text{ns}$ . From (13), we can determine the part that causes  $J_c$  to be periodic is

$$J_{\text{periodic}} = \cos 2\pi 3 \frac{4G}{800} t_1 + \cos 2\pi 9 \frac{4G}{800} t_1 + \dots + \cos 2\pi 759 \frac{4G}{800} t_1 + \dots \quad (15)$$

Since the period of the first term is an integer multiple

of the periods of the remaining terms,  $J_c$  then has a period of  $1/(3.4G) = 66.7\text{ns}$ , which coincides with that shown in Fig. 10.

## CONCLUSION

We have presented the derivation of a generalized complex optimization algorithm for processing frequency-stepped CW measurements. We used two sets of data to compare the performance between the IFFT, the real algorithm, and the complex algorithm. The results demonstrate the resolution enhancement offered by the complex algorithm.

## REFERENCES

- [1] J.L. Eaves and E.K. Reedy, *Principles of Modern Radar*, Van Nostrand Reinhold Company, NY, 1987.
- [2] *HP 8510 Network Analyzer Operating and Programming Manual*, Hewlett-Packard Company, Santa Rosa, CA, 1984.
- [3] G.A. Ybarra et al., "Optimal Signal Processing of Frequency-Stepped CW Radar Data", *IEEE Trans. on Microwave Theory and Techniques*, January, 1995.
- [4] D.G. Luenberger, *Optimization by Vector Space Methods*, Wiley, New York, 1986.
- [5] G.H. Golub and C.F. Van Loan, *Matrix Computations*, Johns Hopkins University Press, Baltimore MD, 1989.
- [6] R.W. Hjellming, "An Introduction to the Radio Astronomy Very Large Array", *National Radio Astronomy Observatory, USA*, 1982.
- [7] W.E.L. Grimson, "A Computational Theory of Visual Surface Interpolation", *Phil. Trans. R. Soc. Lond. B*, vol. 298, pp. 395-422, 1982.
- [8] F.A. Marvasti, *A Unified Approach to Zero-Crossings and Nonuniform Sampling*, EE. Dept., Illinois Institute of Technology Chicago, Illinois, 1987.

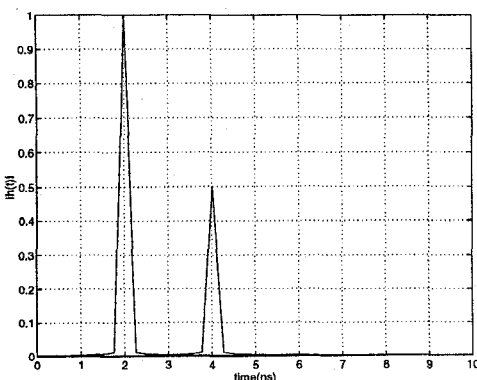


Figure 1: IFFT of 801 reflection coefficients with BW = 4 GHz. The reflections are at  $t_1 = 2.0\text{ns}$ , and  $t_2 = 4.0\text{ns}$

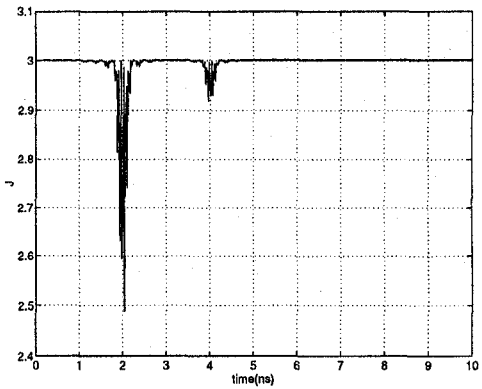


Figure 2: Real amplitude optimized  $J_r$  of 801 reflection coefficients with BW = 4 GHz. The reflections are at  $t_1 = 2.0\text{ns}$ , and  $t_2 = 4.0\text{ns}$

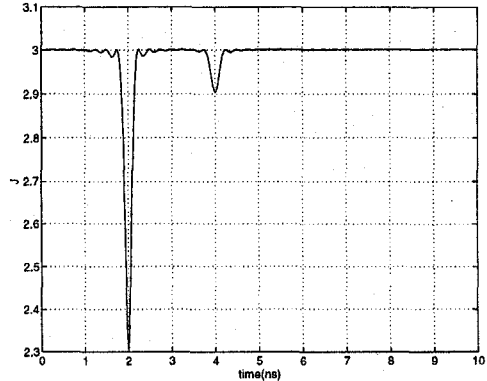


Figure 3: Complex amplitude optimized  $J_c$  of 801 reflection coefficients with BW = 4 GHz. The reflections are at  $t_1 = 2.0\text{ns}$ , and  $t_2 = 4.0\text{ns}$

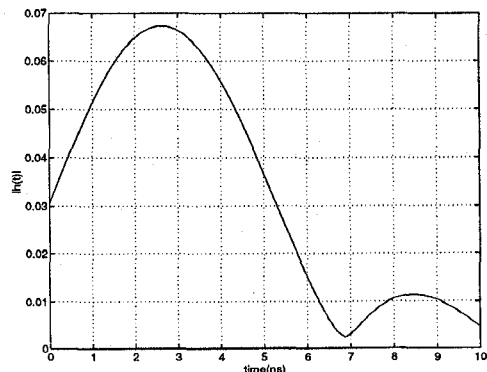


Figure 4: IFFT of 101 measurements of the reflection coefficient with BW = 250 MHz. The reflections are at  $t_1 = 2.0\text{ns}$ , and  $t_2 = 4.0\text{ns}$

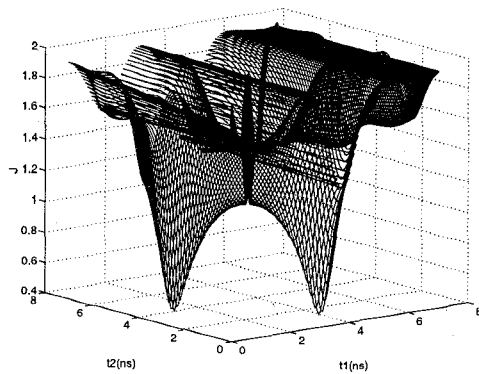


Figure 5: Real amplitude optimized  $J_r$  function of 51 reflection coefficients with BW = 250 MHz. The reflections are at  $t_1 = 2.0\text{ns}$ , and  $t_2 = 4.0\text{ns}$

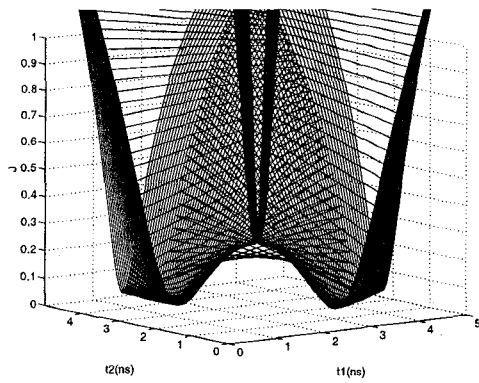


Figure 6: Complex amplitude optimized  $J_c$  function of 51 reflection coefficients with BW = 250 MHz. The reflections are at  $t_1 = 2.0\text{ns}$ , and  $t_2 = 4.0\text{ns}$

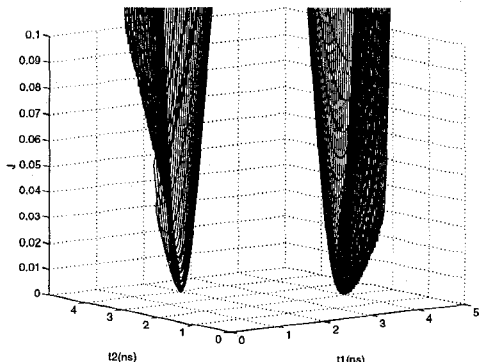


Figure 7: Zoomed complex amplitude optimized  $J_c$  function of 51 reflection coefficients with BW = 250 MHz. The reflections are at  $t_1 = 2.0\text{ns}$ , and  $t_2 = 4.0\text{ns}$

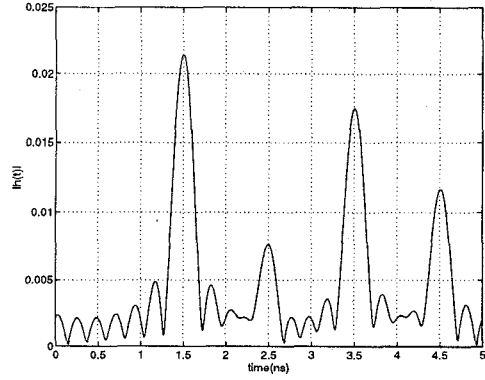


Figure 8: IFFT of 21 uniformly sampled reflection coefficients with BW = 4 GHz. The reflections are at  $t_1 = 1.5\text{ns}$ ,  $t_2 = 3.5\text{ns}$ ,  $t_3 = 4.5\text{ns}$ , and  $t_4 = 7.5\text{ns}$

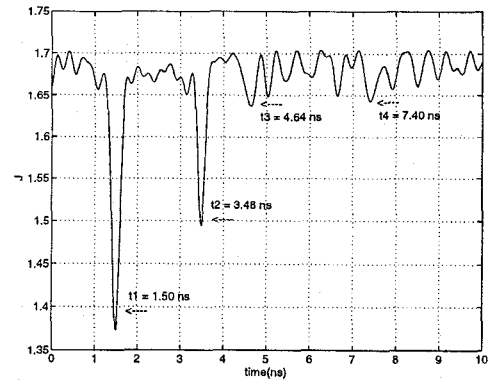


Figure 9: Complex amplitude optimized  $J_c$  function of 23 non-uniformly sampled reflection coefficients. The reflections are at  $t_1 = 1.5\text{ns}$ ,  $t_2 = 3.5\text{ns}$ ,  $t_3 = 4.5\text{ns}$ , and  $t_4 = 7.5\text{ns}$

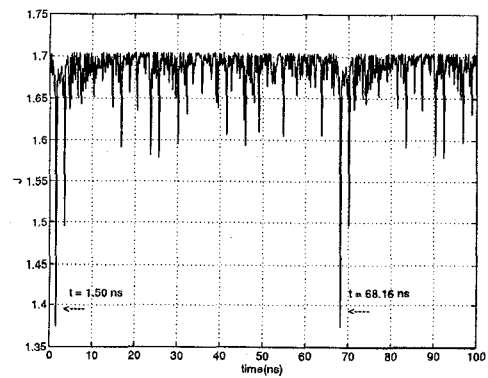


Figure 10: Zoomed complex amplitude optimized  $J_c$  function of 23 non-uniformly sampled reflection coefficients. The reflections are at  $t_1 = 1.5\text{ns}$ ,  $t_2 = 3.5\text{ns}$ ,  $t_3 = 4.5\text{ns}$ , and  $t_4 = 7.5\text{ns}$